Science of the Total Environment 753 (2021) 141791

Contents lists available at ScienceDirect

Science of the Total Environment

journal homepage: www.elsevier.com/locate/scitotenv

Assessing critical load exceedances and ecosystem impacts of anthropogenic nitrogen and sulphur deposition at unmanaged forested catchments in Europe

Martin Forsius [a,*], Maximilian Posch [b], Maria Holmberg [a], Jussi Vuorenmaa [a], Sirpa Kleemola [a], Algirdas Augustaitis [c], Burkhard Beudert [d], Witold Bochenek [e], Nicholas Clarke [f], Heleen A. de Wit [g], Thomas Dirnböck [h], Jane Frey [i], Ulf Grandin [j], Hannele Hakola [k], Johannes Kobler [h], Pavel Krám [l], Antti-Jussi Lindroos [m], Stefan Löfgren [j], Tomasz Pecka [n], Pernilla Rönnback [j], Krzysztof Skotak [n], Józef Szpikowski [o], Liisa Ukonmaanaho [m], Salar Valinia [p], Milan Váňa [q]

[a] Finnish Environment Institute (SYKE), Latokartanonkaari 11, FI-00790 Helsinki, Finland
[b] International Institute for Applied Systems Analysis (IIASA), A-2361 Laxenburg, Austria
[c] Forest Monitoring Laboratory, Vytautas Magnus University, Studentu 13, Kaunas distr. LT-53362, Lithuania
[d] Bavarian Forest National Park, Freyunger Str. 2, D-94481 Grafenau, Germany
[e] Institute of Geography and Spatial Organization, Polish Academy of Sciences, Szymbark 430, 38-311 Szymbark, Poland
[f] Norwegian Institute of Bioeconomy Research, PO Box 115, NO-1431 Ås, Norway
[g] Norwegian Institute for Water Research, Gaustadalléen 21, NO-0349 Oslo, Norway
[h] Environment Agency Austria, Department for Ecosystem Research and Data Information Management, Spittelauer Lände 5, A-1090 Vienna, Austria
[i] Tartu University, Institute of Ecology and Earth Sciences, Vanemuise St. 46, EE-51014 Tartu, Estonia
[j] Swedish University of Agricultural Sciences, PO Box 7050, SE-75007 Uppsala, Sweden
[k] Finnish Meteorological Institute, PO Box 503, FI-00101 Helsinki, Finland
[l] Czech Geological Survey, Department of Geochemistry, Klárov 3, CZ–118 21 Prague 1, Czech Republic
[m] Natural Resources Institute Finland (Luke), Latokartanonkaari 9, FI-00790 Helsinki, Finland
[n] Institute of Environmental Protection – National Research Institute, ul. Kolektorska 4, 01-692 Warsaw, Poland
[o] Adam Mickiewicz University in Poznan, Storkowo 32, 78-450 Grzmiąca, Poland
[p] Swedish Environmental Protection Agency, Climate Department- Air Unit, SE-106 48 Stockholm, Sweden
[q] Czech Hydrometeorological Institute, Observatory Košetice, CZ-394 22 Košetice, Czech Republic

HIGHLIGHTS

- Novel techniques for presenting exceedances of critical loads (CL) and their temporal development were developed.
- Concentrations and fluxes of N and S compounds in deposition and runoff have decreased as a response to decreasing emissions.
- Most sites with higher CL exceedances showed larger decreases in both inorganic N and H^+ concentrations and fluxes in runoff.
- Effects of the cumulative exceedance of the eutrophication CL were evaluated.
- The results provide evidence on the link between CL exceedances and empirical impacts.

GRAPHICAL ABSTRACT

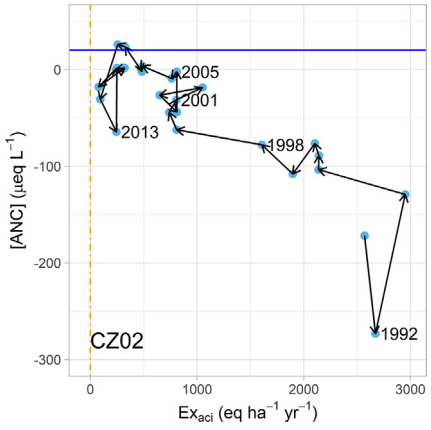

* Corresponding author.
E-mail address: martin.forsius@ymparisto.fi (M. Forsius).

https://doi.org/10.1016/j.scitotenv.2020.141791

ARTICLE INFO

Article history:
Received 8 June 2020
Received in revised form 13 August 2020
Accepted 17 August 2020
Available online 21 August 2020

Editor: Elena Paoletti

Keywords:
Air pollution
Environmental effects
Modelling
Biogeochemistry
Trends

ABSTRACT

Anthropogenic emissions of nitrogen (N) and sulphur (S) compounds and their long-range transport have caused widespread negative impacts on different ecosystems. Critical loads (CLs) are deposition thresholds used to describe the sensitivity of ecosystems to atmospheric deposition. The CL methodology has been a key science-based tool for assessing the environmental consequences of air pollution. We computed CLs for eutrophication and acidification using a European long-term dataset of intensively studied forested ecosystem sites ($n = 17$) in northern and central Europe. The sites belong to the ICP IM and eLTER networks. The link between the site-specific calculations and time-series of CL exceedances and measured site data was evaluated using long-term measurements (1990–2017) for bulk deposition, throughfall and runoff water chemistry. Novel techniques for presenting exceedances of CLs and their temporal development were also developed. Concentrations and fluxes of sulphate, total inorganic nitrogen (TIN) and acidity in deposition substantially decreased at the sites. Decreases in S deposition resulted in statistically significant decreased concentrations and fluxes of sulphate in runoff and decreasing trends of TIN in runoff were more common than increasing trends. The temporal developments of the exceedance of the CLs indicated the more effective reductions of S deposition compared to N at the sites. There was a relation between calculated exceedance of the CLs and measured runoff water concentrations and fluxes, and most sites with higher CL exceedances showed larger decreases in both TIN and H^+ concentrations and fluxes. Sites with higher cumulative exceedance of eutrophication CLs (averaged over 3 and 30 years) generally showed higher TIN concentrations in runoff. The results provided evidence on the link between CL exceedances and empirical impacts, increasing confidence in the methodology used for the European-scale CL calculations. The results also confirm that emission abatement actions are having their intended effects on CL exceedances and ecosystem impacts.

1. Introduction

Anthropogenic emissions of nitrogen (N) and sulphur (S) compounds and their long-range transport have caused widespread impacts on different ecosystems. Nutrient enrichment and imbalances caused by elevated N deposition have been observed over large regions (Bergström et al., 2005; Sutton et al., 2011; Jonard et al., 2015). Impacts on biodiversity in different habitats are also well recognized with documented changes in heathlands and grasslands (Bobbink et al., 2010; Dupre et al., 2010; Stevens et al., 2010), and forest plant communities (Dirnböck et al., 2014; Staude et al., 2020). Deposited S and N has also caused acidification of European and North American lakes and streams (e.g. Wright et al., 2005; Garmo et al., 2014; Liang and Aherne, 2019), and impacts of acidifying deposition on terrestrial ecosystems have also been observed in many regions (Duan et al., 2000a; Sullivan et al., 2012; Oulehle et al., 2017; Johnson et al., 2018).

The accomplished decrease in S emissions is one of the great "success stories" in environmental protection (Sullivan et al., 2018; Grennfelt et al., 2020). European emissions of SO_2 decreased by ca. 60% during 1990–2014, and for NO_x emissions the decrease was about 45% during these years (Fagerli et al., 2016). NH_3 emission reductions have been less successful (decrease by ca. 20% in 1990–2014) due to large emissions mainly from agricultural non-point sources, and in some regions the emissions have even increased slightly.

Even though not all polluting substances have decreased by the required amount, emission reductions have caused decreases in fluxes and concentrations of N and S compounds in deposition and runoff waters of forested ecosystems (Vuorenmaa et al., 2017, 2018) and large-scale chemical (Garmo et al., 2014) and biological (Vrba et al., 2003; Monteith et al., 2005; Lund et al., 2018) recovery of aquatic ecosystems. However, studies have also indicated that it can take a long time before emission abatement measures can be detected as decreases in the acidity of surface waters and soil/soil solutions (Karltun et al., 2003; Wright et al., 2005; Mitchell et al., 2013; Lawrence et al., 2015; Johnson et al., 2018) and biological recovery (Hesthagen et al., 2011). Impacts on less studied components, such as high sensitivity of ectomycorrhizal fungi to N deposition across European forests have also been detected (van der Linde et al., 2018). Moreover, biological recovery in forests to reduced N deposition has not yet been observed (Schmitz et al., 2019). These studies, as well as the well documented impacts of eutrophying N deposition (e.g. Stevens et al., 2010; Dirnböck et al., 2014; Staude et al., 2020) emphasize the importance of continued evaluations of ecosystem responses to deposition impacts, and further developments of associated modelling and assessment methods.

A well-known concept used in the efforts to reduce the air pollution problem is the calculation of critical loads. A critical load (CL) is defined as "a quantitative estimate of an exposure to one or more pollutants below which significant harmful effects on specified sensitive elements of the environment do not occur according to present knowledge" (Nilsson and Grennfelt, 1988). The CL concept has been used in policy negotiations by both the EU Commission and the Convention on Long-range Transboundary Air Pollution (CLRTAP), in which European maps of CLs and critical levels have been used to optimise emission reductions by connecting costs for reductions measures, emission scenarios, deposition and air quality modelling and CLs (RAINS/GAINS integrated assessment modelling) (Amann et al., 2011; Posch et al., 2012; de Vries et al., 2015; Grennfelt et al., 2020). In 2017, CLs for eutrophication were exceeded in about 64% of the ecosystem area in Europe, the comparable figure for acidification being about 6% (Fagerli et al., 2019). The CLs approach has also been used for air pollution assessment in many other regions of the world (Duan et al., 2000a, 2000b; Ouimet et al., 2006; Zhao et al., 2007; Forsius et al., 2010; Josipovic et al., 2011; Pardo et al., 2011). Other quantitative approaches for assessing impacts of N and S deposition have also recently been proposed, including an indicator for integrated cumulative N exceedance (Rowe et al., 2017) and target loads for acidic deposition (Posch et al., 2019).

The aim of this study is to i) compute CLs for eutrophication and acidification of intensively studied forested ecosystem sites ($n = 17$) in Europe, ii) present exceedances of CLs in a novel way displaying time-series of measured deposition, and iii) assess the link between the site-specific calculations and time-series of CL exceedance (using both measured and modelled deposition) and a measured impact indicator indicating long-term responses (surface water chemistry). Testing and developing the impacts concepts used in the policy work for deriving European emission reduction agreements is a key task. The studied sites cover a large gradient of deposition loads, climatic conditions and sensitivity to deposition impacts, and are part of networks of ICP Integrated Monitoring (e.g. Vuorenmaa et al., 2017, 2018) and eLTER (Holmberg et al., 2018; Mirtl et al., 2018). The study is an extension and update of a previous article on this topic (Holmberg et al., 2013), by improving and extending the empirical database and introducing new calculation and evaluation methods.

2. Material and methods

2.1. Sites, data collection and statistical methods

The data set of this study has been collected in the ICP Integrated Monitoring (ICP IM) network, set up for the assessment and monitoring of air pollution effects under CLRTAP (www.syke.fi/nature/icpim). Most of the sites are also part of the European ecosystem research infrastructure eLTER. Data from 17 ICP IM sites in northern and central Europe from the period 1990–2017 were used (Table 1). The monitoring network as well as methods for sampling and analysis have been described in detail elsewhere (Manual for Integrated Monitoring, 2013; Vuorenmaa et al., 2017, 2018) and are here only briefly summarised. Information on sampling methods, data treatment and statistical methods is also given in the Supplementary Material (section C).

The ICP IM sites are in nature conservation areas or similar semi-natural locations and receive different loads of atmospheric deposition (Fig. 1). The predominant habitat is coniferous and broadleaf forests, and some sites also contain lakes (Table 1). Monitoring is intensive and covers different ecosystem compartments in order to provide information for studying long-term trends, element fluxes and cause-effect relationships (Manual for Integrated Monitoring, 2013). The locations of the sites considered in this paper are shown in Fig. 1 (left). They are overlaid with the exceedance of the European critical loads for eutrophication (see Hettelingh et al., 2017) under the 2015 N deposition. To illustrate the amount of N deposited at the sites, the right map in Fig. 1 shows the cumulative total N deposition in Europe for the period 1880–2020 (earlier depositions updated from Schöpp et al., 2003).

In the present paper we use long-term data for bulk and throughfall deposition and surface water quality, as well as catchment information for the CL calculations (Section 2.2) from the sites. Trends for bulk deposition (BD) and runoff were evaluated for annual mean concentrations (μeq L^{-1}) and annual fluxes (meq m^{-2} yr^{-1}) of nitrate (NO_3-N), ammonium (NH_4-N), total inorganic nitrogen (TIN = NO_3-N + NH_4-N), non-marine sulphate (xSO_4), hydrogen ion (H^+, effective concentration only) and ANC (Acid Neutralising Capacity, ANC = $[Ca^{2+} + Mg^{2+} + Na^+ + K^+] - [SO_4^{2-} + NO_3^- + Cl^-]$). Total deposition of xSO_4 and TIN was estimated from the BD and throughfall measurements by calculating the annual deposition to the open area (BD) and the forest area (throughfall), and then estimating area-weighted deposition (see Supplementary Material and Vuorenmaa et al., 2018 for details).

We used the well-established non-parametric Mann-Kendall test (MKT) (Gilbert, 1987; Libiseller and Grimvall, 2002) applied to annual data for trend detection and the Theil-Sen method (Sen, 1968) for slope estimation (Supplementary Material). A statistical significance threshold of $p < 0.05$ was applied.

2.2. Calculation of critical loads of eutrophication and acidity and their exceedances

Critical loads (CLs) of both eutrophication and acidity were calculated for the sites. The derivation of these CLs from mass and charge balance models is given in the Mapping Manual of the ICP M&M (www.umweltbundesamt.de/en/Coordination_Centre_for_Effects) and in Posch et al. (2015a). Details on the methods used in the present study are given in the Supplementary Material.

The critical load of nutrient N, $CL_{nut}N$, is derived from the N mass balance for an acceptable (critical) N leaching. The site-specific (catchment-scale) acceptable N concentrations $[N]_{acc}$ (in mg L^{-1}) were based on the suggested values in the Manual (Table V.5) to avoid

Table 1
Catchment characteristics of the 17 studied ICP IM sites. The sites belonging also to the eLTER network are indicated.

Site code	Site name	Country	eLTER	Catchment area (km^2)	Altitude (m)	Forest area (%)	Lake surface area (%)	Peat soil area (%)	Predominant vegetation	Dominant bedrocks	Soil type
AT01	Zöbelboden	Austria	x	0.90	550–950	100	0	0	Norway spruce, European beech	Calcitic dolomite	Chromic Cambisols, Hydromorphic Stagnosols, Lithic and Rendzic Leptosols
CZ01	Anenske Povodi	Czech Republic		0.29	487–543	90	0	0	Norway spruce	Biotitic and sillimanitic-biotitic paragneiss	Dystric Cambisols
CZ02	Lysina	Czech Republic	x	0.27	829–949	100	0	0	Norway spruce	Leucogranite	Podzol, Gleysol
DE01	Forellenbach	Germany	x	0.69	787–1293	95	0	30	Norway spruce, European beech	Granite, gneiss	Dystric and Podzolic Cambisols, Rankers and Lithosols
EE02	Saarejärve	Estonia	x	3.32	44–77	68	8	10	Norway spruce, Scots pine	Sandstone, limestone	Haplic Podzol, glaciofluvial sands
FI01	Valkea-Kotinen	Finland	x	0.30	150–190	86	13	19	Norway spruce, Scots pine	Mica gneiss	Dystric Cambisols, Histols
FI03	Hietajärvi	Finland		4.64	165–214	55	23	35	Scots pine dominated	Porphyritic granodiorites	Fibric Histosols, Podzols
LT01	Aukstaitija	Lithuania	x	1.02	159–189	100	0	10	Norway spruce, Scots pine	Sandstone, limestone	Podzols
LT03	Zemaitija	Lithuania	x	1.47	147–180	100	0	20	Norway spruce, Scots pine	Sandstone, limestone	Podzols
NO01	Birkenes	Norway	x	0.41	200–300	90	0	7	Norway spruce, Scots pine	Granite	Podzols, Histosols, Leptosols
NO02	Kårvatn	Norway	x	25	200–1375	18	4	2	Scots pine, alpine birch	Gneiss, quartzite	Podzols
PL06	Storkowo	Poland		74.3	83–203	41	0.3	1.7	Scots pine	Sand, loamy sand	Podzols
PL10	Szymbark	Poland		13	301–753	38	0	0	European beech, fir	Sandstone, shale	Dystric and Eutric Cambisols
SE04	Gårdsjön	Sweden	x	0.04	114–140	95	0	10	Norway spruce	Granite	Podzol, Histosols
SE14	Aneboda	Sweden	x	0.19	210–240	99	0	17	Norway spruce, Scots pine	Granite	Podzol, Gleysols, Histosols
SE15	Kindla	Sweden	x	0.20	312–415	99	0	24	Norway spruce	Granite	Podzol, Histosols
SE16	Gammtratten	Sweden	x	0.45	410–545	99	0	16	Norway spruce, Scots pine	Granite	Podzol, Histosols

impacts on forests such as nutrient imbalances and vegetation changes (range used: 0.3–5.2 mg L^{-1}). Long-term net N immobilisation was set to 0.5 kg ha^{-1} yr^{-1} (Mapping Manual, section V.3.1.3.1) and N uptake was assumed zero for all sites, as no harvesting took place there. Finally, the denitrification fraction was calculated as $f_{de} = 0.1 + 0.7 \cdot f_{peat}$, where f_{peat} is the fraction of peatland in the catchment (Posch et al., 1997). Empirical critical loads of nitrogen, $CL_{emp}N$, were set to the minimum of the range proposed in Bobbink and Hettelingh (2011) for the respective ecosystem types (EUNIS classes) present at each site (Holmberg et al., 2013, range used 5–10 kg ha^{-1} yr^{-1}). The eutrophication critical load, $CL_{eut}N$, was then determined as the minimum of $CL_{nut}N$ *and* $CL_{emp}N$.

Acidity in a soil/surface water is determined by both N and S deposition. Thus, an acidity CL is not a single value, but given by a critical load function (CLF), characterized by values such as $CL_{max}S$ and $CL_{max}N$ (see Supplementary Material). For the study catchments, these values were determined for surface waters by using the FAB model (Henriksen and Posch, 2001; see also Mapping Manual and Posch et al., 2012). As chemical criterion the ANC was used with the value $[ANC]_{limit} = 20$ μeq L^{-1}. This limit value has been shown to protect fish in downstream habitats (Lien et al., 1996). For the sites containing lakes, the in-lake retention was calculated using net mass transfer coefficient values $s_N = 6.5$ m yr^{-1} and $s_S = 0.5$ m yr^{-1} for N and S, respectively (after Kaste and Dillon, 2003; Baker and Brezonik, 1988). Arithmetic average of the annual runoff sums was used in the calculations. To calculate the pre-acidification base cation concentration, the coefficients $a = 8$ μeq L^{-1}, $b = 0.17$ were used, and the so-called F-factor was set to the value of one for base cation concentrations above 400 μeq L^{-1} (Brakke et al., 1990; Henriksen and Posch, 2001). Finally, we also considered the N-S critical load function, derived by intersecting the $CL_{eut}N$-line with the acidity CLF. Non-exceedance of the resulting CLF means that neither eutrophication nor acidity criterion are violated.

The N and S depositions at the sites were obtained from measured site data (see Section 2.1). Finally, we also studied the relationship over time between CL exceedances and (critical) chemical variables (TIN and ANC) at the sites. For $CL_{eut}N$ the relationship between the TIN concentration and the cumulative exceedance of $CL_{eut}N$ (over 3 and 30 years) was also studied, as it is argued that not the deposition in a single year, but its accumulation over a certain period better explains its impact on ecosystems (Rowe et al., 2017).

3. Results and discussion

3.1. Observed changes in deposition and water quality at the ICP IM sites

The large decreases in European S emissions are clearly reflected in the observations at the ICP IM sites. Statistically significant decreasing trends in both fluxes and concentrations of xSO_4 in bulk and total deposition as well as runoff water (RW) are totally dominating (Table 2). Deposition trends of TIN and NH_4 are also decreasing, but the number of statistically significant trends is lower than for xSO_4. Acidity in precipitation and runoff water has substantially decreased at the sites (Table 2). Decreasing trends of concentrations and fluxes of TIN in runoff are more commonly observed than increasing trends, particularly for NO_3. TIN concentrations in runoff water declined at 14 out of 17 sites. These results confirm earlier detailed evaluations of trends and mass balances at the ICP IM sites (Vuorenmaa et al., 2017, 2018). According to Vuorenmaa et al. (2018), the number of statistically significant decreasing trends have increased during the last 25 years, but that the change now is slowing down.

The mass budget studies of these sites (Vuorenmaa et al., 2017) have also shown that the S input-output budget is now in balance or show S release whereas N compounds in general still showed efficient catchment retention. The exception were sites impacted by disturbances caused by storm-felling and bark beetle infestation (Löfgren et al., 2011, 2014; Beudert et al., 2014). Earlier studies have furthermore indicated the changes in the N and S mass budgets also affect the H^+ (proton) budgets at these sites (Forsius et al., 2005).

3.2. Critical loads of eutrophication and acidity and their exceedance

For the 17 ICP IM sites the eutrophication CL ($CL_{eut}N$), the N (TIN) deposition (measured) at the site for the year 2017 and its exceedance ($Ex_{eut} = \max\{N_{dep}\text{-}CL_{eut}N, 0\}$) are given in Table 3. Similarly, the acidity CL-function (CLF, defined by $CL_{max}N$, $CL_{max}S$ and CLS_1), the measured total S (xSO_4) deposition (see 2.1 for methods description) at the site for the year 2017 and their exceedances (Ex_{aci} = exceedance of the critical load of acidity) are shown. Also, $CL_{min}S$ of the N-S CL-function, obtained by intersecting $CL_{eut}N$ with the acidity CL-function (see below) is given for every site, together with its exceedance Ex_{NS}. The methods

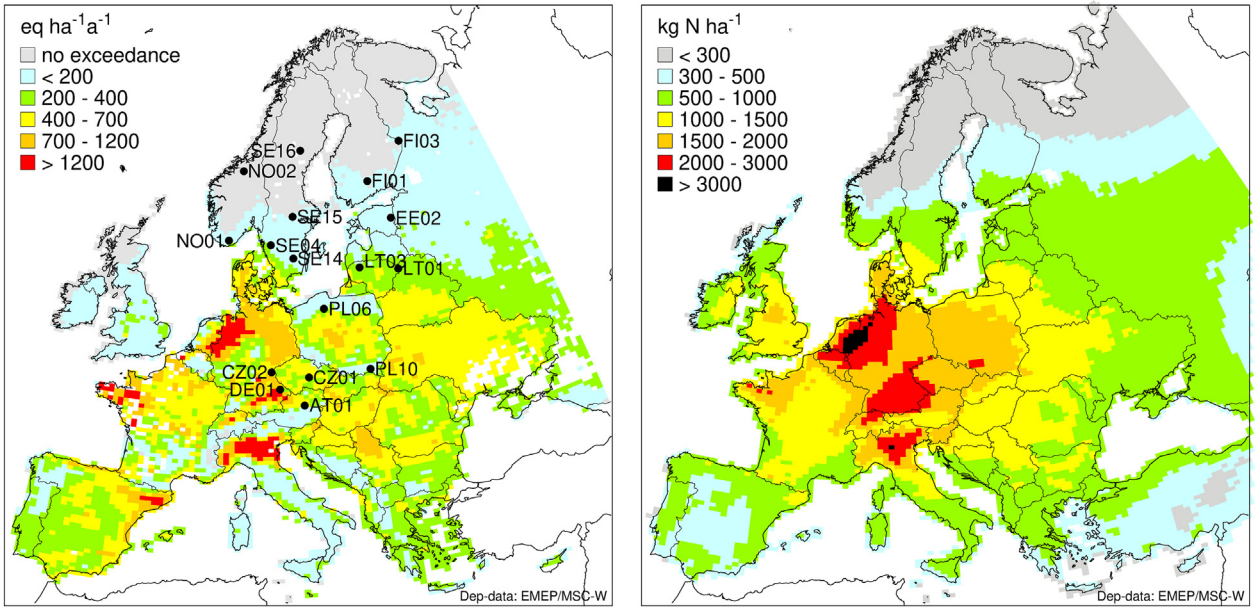

Fig. 1. Locations of the 17 ICP IM sites considered in this paper (left). On the background map the 2015 average accumulated exceedance (AAE, in eq ha^{-1} yr^{-1}) of the European critical loads of eutrophication is shown. Right: The modelled cumulative deposition of total nitrogen ($NO_x + NH_3$) for the period 1880–2020 in Europe.

Table 2
Temporal trends (1990–2017) in bulk deposition (BD) and runoff water (RW) for annual mean concentrations (denoted as *c*) and annual fluxes (*f*) for non-marine sulphate (xSO_4), nitrate (NO_3), ammonium (NH_4), total inorganic nitrogen (TIN=NO_3 + NH_4), hydrogen ions (H^+) and ANC (RW only) in the 17 studied IM catchments. Total deposition to the forest floor of xSO_4 and TIN is denoted as xSO_4tot*f* and TINtot*f*, respectively. For the annual change, a significant trend ($p < 0.05$) is presented in bold. Annual changes and their mean and median (Md.) values for concentrations and fluxes are given in μeq L^{-1} yr^{-1} and meq m^{-2} yr^{-1}, respectively.

Site	Prog.	Data	xSO_4c	NO_3c	NH_4c	TINc	H^+	ANCc	xSO_4f	xSO_4totf	NO_3f	NH_4f	TIN *f*	TIN tot *f*
				μeq L^{-1}					meq m^{-2} yr^{-1}					
AT01	BD	1993–2017	**−0.79**	**−0.32**	0.01	−0.16	**−0.69**	–	**−1.18**	**−1.26**	−0.38	0.25	0.21	−0.49
	RW	1995–2017	**−2.06**	0.80	0.00	0.77	**0.00**	**12.4**	**−0.89**	–	0.55	0.00	0.55	–
CZ01	BD	1990–2017	**−2.37**	**−0.91**	**−0.75**	**−1.63**	**−1.64**	–	**−1.48**	**−4.49**	**−0.53**	−0.28	**−0.80**	−0.33
	RW	1990–2017	−2.75	**−2.09**	**−0.09**	**−2.33**	−0.00	4.95	−0.67	–	**−0.13**	**−0.01**	**−0.15**	–
CZ02	BD	1991–2017	**−2.06**	**−0.83**	**−0.83**	**−1.73**	**−1.28**	–	**−1.89**	**−7.47**	**−0.79**	**−0.95**	**−1.82**	**−1.62**
	RW	1990–2017	**−13.4**	**−1.03**	**0.01**	**−1.03**	**−1.54**	**6.75**	**−6.07**	–	**−0.51**	0.00	**−0.51**	–
DE01	BD	1991–2017	**−1.12**	**−0.55**	**−0.43**	**−0.99**	**−1.00**	–	**−1.50**	**−2.35**	**−0.72**	**−0.72**	**−1.45**	−0.46
	RW	1991–2017	**−0.93**	−0.28	**−0.14**	−0.40	**−0.02**	**3.55**	**−1.15**	–	−0.53	**−0.14**	−0.64	–
EE02	BD	1994–2017	**−1.48**	**−0.50**	**−0.71**	**−1.40**	−0.13	–	**−0.91**	**−1.61**	**−0.27**	**−0.40**	**−0.56**	**−0.50**
	RW	1994–2017	**−12.5**	−0.05	−0.05	−0.17	−0.00	**39.2**	−0.23	–	0.19	0.03	0.21	–
FI01	BD	1990–2017	**−0.88**	**−0.20**	**−0.22**	**−0.45**	**−0.72**	–	**−0.62**	**−1.15**	**−0.15**	**−0.16**	**−0.33**	**−0.20**
	RW	1990–2017	**−2.72**	−0.02	−0.04	−0.05	**−0.55**	**0.80**	**−0.63**	–	−0.01	−0.01	−0.02	–
FI03	BD	1990–2017	**−0.83**	**−0.19**	**−0.14**	**−0.42**	**−0.74**	–	**−0.44**	**−0.54**	**−0.11**	−0.04	**−0.16**	−0.06
	RW	1990–2017	**−0.75**	−0.01	**−0.02**	**−0.03**	−0.01	**0.84**	**−0.27**	–	0.00	**−0.01**	−0.01	–
LT01	BD	1993–2017	**−1.63**	**−0.77**	−0.75	**−1.68**	−0.10	–	**−1.10**	**−1.43**	**−0.50**	**−0.64**	**−1.05**	**−1.30**
	RW	1994–2017	**−42.5**	**−0.28**	−0.01	−0.33	**−0.00**	9.95	**−6.68**	–	−0.01	0.00	−0.01	–
LT03	BD	1995–2017	**−1.78**	**−0.95**	−0.56	**−1.73**	0.19	–	**−1.64**	**−3.40**	**−0.69**	−0.29	**−1.25**	**−1.97**
	RW	1996–2017	**−32.3**	**−0.41**	−0.05	**−0.43**	0.00	−2.29	−1.17	–	0.01	0.02	0.03	–
NO01	BD	1990–2017	**−1.22**	**−0.59**	**−0.49**	**−1.05**	**−1.18**	–	**−1.51**	**−2.80**	−0.30	−0.20	−0.52	**−1.19**
	RW	1990–2017	**−2.88**	−0.11	–	−0.11	**−0.40**	**2.19**	**−3.00**	–	−0.08	–	−0.08	–
NO02	BD	1990–2017	**−0.11**	0.03	0.05	**0.12**	**−0.19**	–	**−0.19**	**−0.20**	0.02	0.08	0.12	0.15
	RW	1990–2017	**−0.18**	**−0.03**	–	**−0.03**	**−0.01**	**0.74**	**−0.31**	–	**−0.03**	–	**−0.03**	–
PL06	BD	1995–2017	**−1.85**	**−0.69**	**−1.25**	**−2.09**	**−1.17**	–	**−1.46**	**−1.96**	**−0.54**	**−1.04**	**−1.82**	−0.42
	RW	1995–2017	**−11.4**	**−1.70**	**−0.64**	**−2.82**	0.00	**25.6**	**−4.84**	–	**−0.95**	**−0.30**	**−1.36**	–
PL10	BD	1995–2017	−0.51	−0.48	**−1.00**	**−1.71**	**−0.90**	–	−0.42	−0.30	−0.33	**−0.74**	**−1.02**	−0.87
	RW	1993–2017	−6.37	**−1.36**	0.32	**−1.59**	**0.00**	−11.6	−8.03	–	**−1.67**	−0.14	**−1.74**	–
SE04	BD	1990–2017	**−1.33**	**−0.54**	**−0.44**	**−0.98**	**−1.22**	–	**−1.31**	**−2.94**	**−0.47**	**−0.51**	**−0.89**	**−1.67**
	RW	1990–2017	**−8.30**	0.02	0.01	0.03	**−1.41**	**4.67**	**−4.06**	–	**0.03**	0.02	**0.04**	–
SE14	BD	1996–2017	**−0.95**	**−0.63**	**−0.48**	**−1.08**	**−1.05**	–	**−0.93**	**−1.17**	**−0.96**	**−0.79**	**−1.70**	**0.35**
	RW	1996–2017	**−4.59**	**0.45**	0.01	**0.51**	**−1.07**	**2.06**	**−2.14**	–	**0.19**	0.00	**0.21**	–
SE15	BD	1996–2017	**−0.91**	**−0.52**	**−0.39**	**−0.87**	**−1.02**	–	**−0.78**	**−1.34**	**−0.38**	−0.31	**−0.57**	**−0.65**
	RW	1996–2017	**−4.44**	−0.02	0.00	−0.01	**−0.78**	**2.59**	**−2.37**	–	−0.01	0.00	−0.01	–
SE16	BD	1996–2017	**−0.52**	**−0.24**	−0.23	**−0.46**	**−0.43**	–	**−0.46**	**−0.38**	**−0.29**	**−0.29**	**−0.58**	**−0.31**
	RW	1996–2017	**−0.98**	**−0.06**	−0.01	**−0.08**	−0.03	0.78	−0.50	–	−0.01	−0.01	−0.02	–
Mean	BD		−1.20	−0.52	−0.51	−1.08	−0.78	–	−1.05	−2.05	−0.43	−0.41	−0.84	−0.68
Md.	BD		−1.12	−0.54	−0.48	−1.05	−0.34	–	−1.18	−1.61	−0.38	−0.28	−0.56	−0.46
Mean	RW		−8.77	−0.36	−0.05	−0.48	−0.90	6.07	−2.53	–	−0.18	−0.04	−0.21	–
Md.	RW		−4.44	−0.06	−0.01	−0.11	−0.01	2.59	−1.17	–	−0.01	0.00	−0.02	–

for calculating those exceedances are described in the Supplementary Material.

CL exceedance is depending on both the sensitivity of the site and the deposition load to the system. For three sites (NO01, SE04 and SE15), $CL_{eut}N$ is greater than $CL_{max}N$ (and thus $CL_{min}S = 0$), i.e. the N-S CL-function is the same as the acidity CLF (and thus $Ex_{aci} = Ex_{NS}$) (Table 3). At eight sites neither $CL_{eut}N$ nor the acidity CLF is exceeded; at three sites both CLs are exceeded; at four sites the acidity CL is not

Table 3
Critical loads of eutrophication ($CL_{eut}N$) and acidity ($CL_{max}N$, $CL_{max}S$ and CLS_1, defining the CL-function) and their exceedances (Ex_{eut}, Ex_{aci}) for 2017 measured total N (N_{dep}) and S (S_{dep}) depositions (all in eq ha^{-1} yr^{-1}) at the 17 ICP IM sites. Also given is $CL_{min}S$, obtained by intersection $CL_{eut}N$ with the acidity CLF and Ex_{NS}, the exceedance for this combined N-S CL-function (see text for details). Note that figures are rounded to integers and presented with three significant digits.

Site	N_{dep}	S_{dep}	$CL_{eut}N$	$CL_{max}N$	$CL_{max}S$	CLS_1	$CL_{min}S$	Ex_{eut}	Ex_{aci}	Ex_{NS}
eq ha^{-1} yr^{-1}										
AT01	1180	143	714	19,500	17,500	17,500	16,900	1060	0	1060
CZ01	656	288	193	300	244	241	99	464	644	652
CZ02	542	199	282	513	409	409	198	260	240	261
DE01	487	77	509	2990	2090	2080	1750	0	0	0
EE02	150	82	495	38,600	13,000	13,000	12,900	0	0	0
FI01	165	63	239	2060	373	372	336	0	0	0
FI03	131	62	357	2960	653	648	581	0	0	0
LT01	345	95	357	5300	4370	4370	4110	0	0	0
LT03	358	104	357	4570	3450	3450	3200	1	0	1
NO01	943	179	357	256	194	191	0	586	866	866
NO02	152	62	357	448	380	355	84	0	0	0
PL06	481	131	195	11,400	10,200	10,200	10,000	286	0	286
PL10	837	572	290	11,000	10,600	10,500	10,300	547	0	547
SE04	509	62	525	370	282	281	0	0	200	200
SE14	228	47	237	584	430	429	272	0	0	0
SE15	296	37	357	284	183	183	0	0	51	51
SE16	91	36	340	555	411	410	170	0	0	0

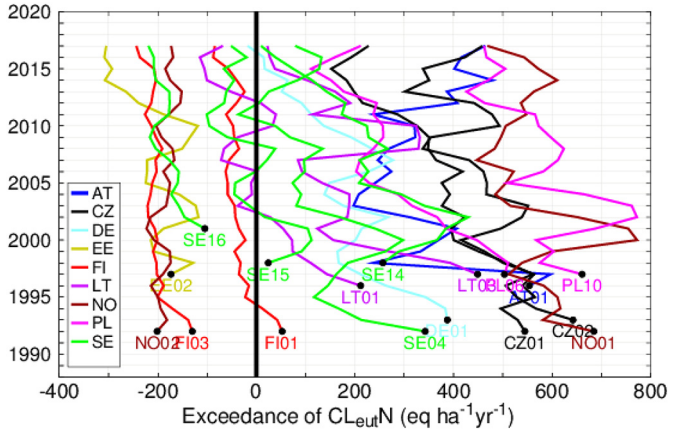

Fig. 2. Exceedance of eutrophication critical loads ($CL_{eut}N$) over time at the 17 ICP IM sites using the total N deposition measurements at the sites. A three-year moving average of depositions has been used to increase clarity. Negative numbers indicate non-exceedance.

exceeded, but $CL_{eut}N$ is; and at two sites (SE04, SE15) $CL_{eut}N$ is not exceeded, but the acidity CL is.

We have developed different ways to illustrate exceedances of CLs and their temporal development. The temporal development of the exceedance of the eutrophication CL ($CL_{eut}N$) is a simple case since the CL is given by a single number (Fig. 2). A 3-year moving average N deposition (last 3 years for a given year) has been used to increase clarity.

The observed decrease in N deposition at the ICP IM sites has been clearly smaller than for S (Table 2), which is reflected also in the temporal development of Ex_{eut} (Fig. 2). Also European scale calculations indicate that exceedance of the eutrophication CL remains a large-scale problem (Fig. 1, Hettelingh et al., 2017), with about 64% of the ecosystem area in Europe exceeded in 2017 (Fagerli et al., 2019).

For acidity CLs, characterized by the quantities $CL_{max}N$, $CL_{max}S$, N_i and CLS_1 forming the CL-function (CLF), it is more complicated to illustrate exceedances in two dimensions. One alternative is to plot all the deposition pairs, relative to one 'normalized' CLF (Fig. 3a). From this figure one can clearly see which site has a positive exceedance, and also how large this exceedance is compared to the CL values. The relative position of N_{dep}, x_N, and S_{dep}, y_S, for a site is calculated as:

$$x_N = \begin{cases} N_{dep}/N_i & \text{if } N_{dep} \le N_i \\ 1 + (N_{dep} - N_i)/(CL_{max}N - N_i) & \text{else} \end{cases}$$
$$y_S = S_{dep}/CLS_1 \qquad (1)$$

In Fig. 3a a 'normalized' CLF is shown, and all deposition pairs relative to it, as if that CLF was the one of the respective site. Of course, it is impossible to write concrete numbers to the axes of the plot, but from x_N and y_S the actual values N_{dep} and S_{dep} can always be recalculated for every site by inverting Eq. (1) and using the CL-values from Table 3. The graph does not show whether a site has a higher deposition than another one, but it gives a good impression by how much (compared to its respective CL-function) CLs are exceeded (or not).

Using the relative exceedances (Eq. (1) and Fig. 3a), also the exceedance history of acidity CLs can be shown (Fig. 3b). Although deposition paths are smoothed in the figure, the graph remains difficult to read. This is caused by the fact that 2017 deposition ends for most sites close to zero for S (when compared to $CL_{max}S$) and close to N_i for N

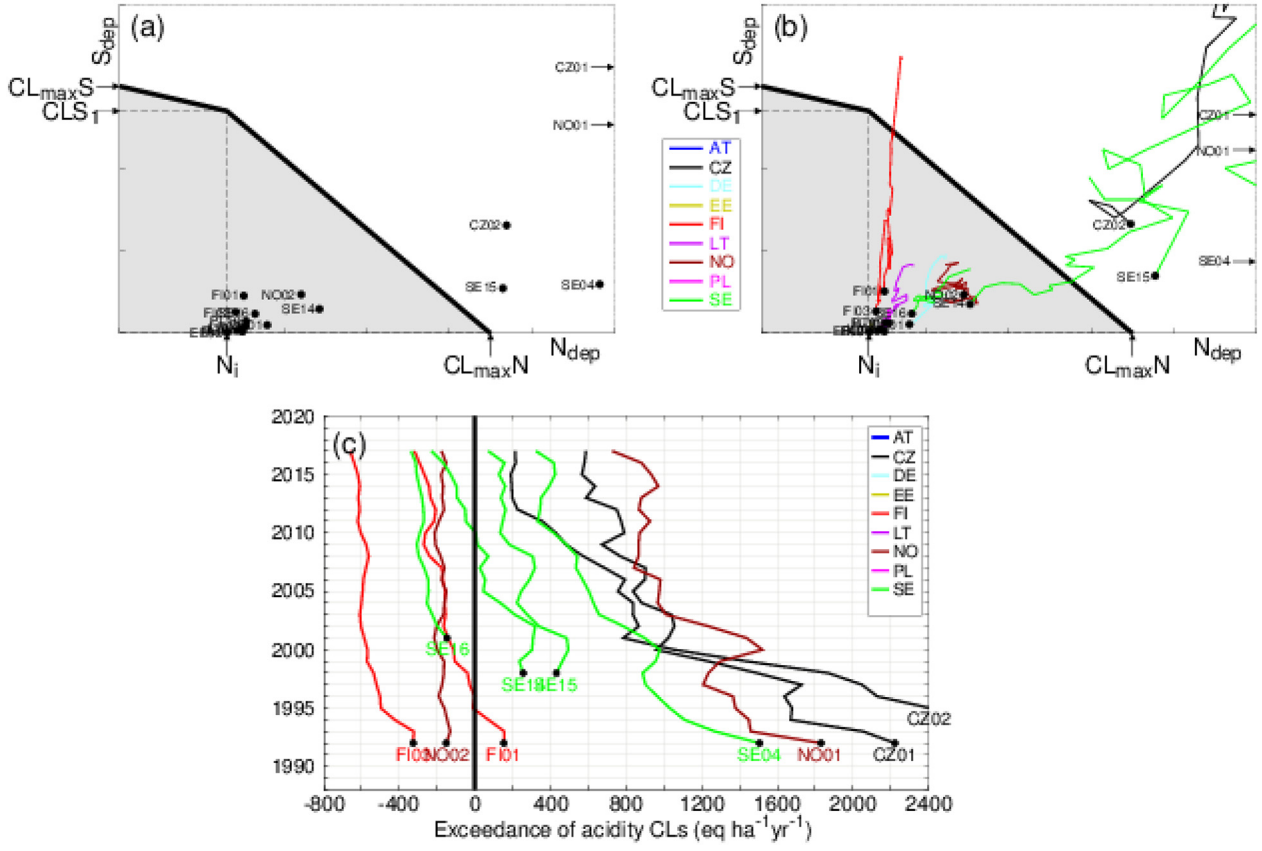

Fig. 3. Exceedance of the critical load of acidity at the 17 ICP IM sites: (a) Acidity CLF for the sites and their normalized depositions in 2017 (Note: for two sites the N deposition is too far beyond its respective $CL_{max}N$); (b) Temporal development of the exceedances of acidity critical loads at the sites using all total N and S deposition measurements at the sites (3-year moving average); (c) Exceedance of acidity critical loads (CLF) over time (vertical axis) at the sites, using the total N and S deposition measurements (3-year moving average) at the sites. Negative numbers indicate non-exceedance. Note that for 7 sites (AT01, DE01, EE02, LT01, LT03, PL06, PL10) the non-exceedance paths are outside to the left.

deposition. An alternative is thus a graph similar to Fig. 2 by plotting acidity exceedance on the x-axis versus time (vertical axis). This requires deriving formulae for computing negative exceedance numbers when the (N,S) deposition pair lies below the CLF. This can be done in an analogous way as for positive exceedance, by also computing the shortest distance to the CLF (from below) and by assigning the x- and y-component of the connecting line as the (negative!) N and S-exceedance (see Supplementary Material for technical details). A three-year moving average of total measured N and S deposition has been used to increase clarity (Fig. 3c).

The temporal development of the exceedance of acidity CLs (Fig. 3c) clearly shows the more effective reductions of S deposition compared to N at the ICP IM sites (Table 2). In 2017, acidity CLs were exceeded in only about 6% of the ecosystem area in Europe (Fagerli et al., 2019).

It should be recognized that CL calculations are based on steady-state assumptions, but in ecosystem processes such as forest growth, soil cation exchange, and climate change are causing dynamic responses in the catchments to the changing deposition inputs. A CL could thus be exceeded but the site not yet damaged, or the CL could be no longer exceeded but the site not yet recovered (Posch et al., 2019). Both modelling studies (Wright et al., 2005; Dirnböck et al., 2018; Posch et al., 2019) and empirical data (Mitchell et al., 2013; Johnson et al., 2018; Vuorenmaa et al., 2018) indicate long time lags between emission reductions and ecosystem responses. This issue is discussed further in Section 3.4 below.

3.3. Single critical load function for N and S

It has been a common practise to estimate separate CLs of acidity and eutrophication (e.g. Hettelingh et al., 2017). However, if a site is impacted by both eutrophying and acidifying deposition, the chemical criteria for both effects can be considered at the same time, deriving a single critical load function for N and S (Fig. 4a; see also Posch et al., 2015a and Supplementary Material).

The value of $CL_{min}S$ is obtained as (if $N_i < CL_{eut}N < CL_{max}N$; otherwise $CL_{min}S = CLS_1$ or $= 0$, resp.):

$$CL_{min}S = CLS_1 \frac{CL_{max}N - CL_{eut}N}{CL_{max}N - N_i} \quad (2)$$

Again, one can plot all the deposition pairs, relative to a 'normalized' N-S CLF. The relative depositions of x_N and y_S of N_{dep} and S_{dep}, resp., are computed in a similar fashion as above (Eq. (1)). The equations for x_N is in this case:

$$x_N = \begin{cases} N_{dep}/N_i & \text{if } N_{dep} \le N_i \\ 1 + (N_{dep} - N_i)/(CL_{eut}N - N_i) & \text{else} \end{cases} \quad (3)$$

Assuming that $CL_{eut}N < CL_{max}N$ (otherwise Eq. (1) applies). And y_S is calculated as in the case of acidity: $y_S = S_{dep}/CLS_1$. In Fig. 4b relative exceedances of the N-S CLF are shown for the 2017 depositions (compare Fig. 3). From x_N and y_S the actual values N_{dep} and S_{dep} can always be re-calculated for every site (using the CL-values from Table 3). Furthermore, in Fig. 4c we show the temporal development of the exceedance of the N-S critical loads (see Supplementary Material for exceedance calculations) again using a 3-year moving average of N and S deposition.

Again, not many sites change from exceedance to non-exceedance of N-S CLs over time; the exceptions are sites FI01 are LT01, with sites DE01, LT03 and SE14 approaching non-exceedance in 2017 (Fig. 4c). Examples of large-scale applications for Europe and China of the single

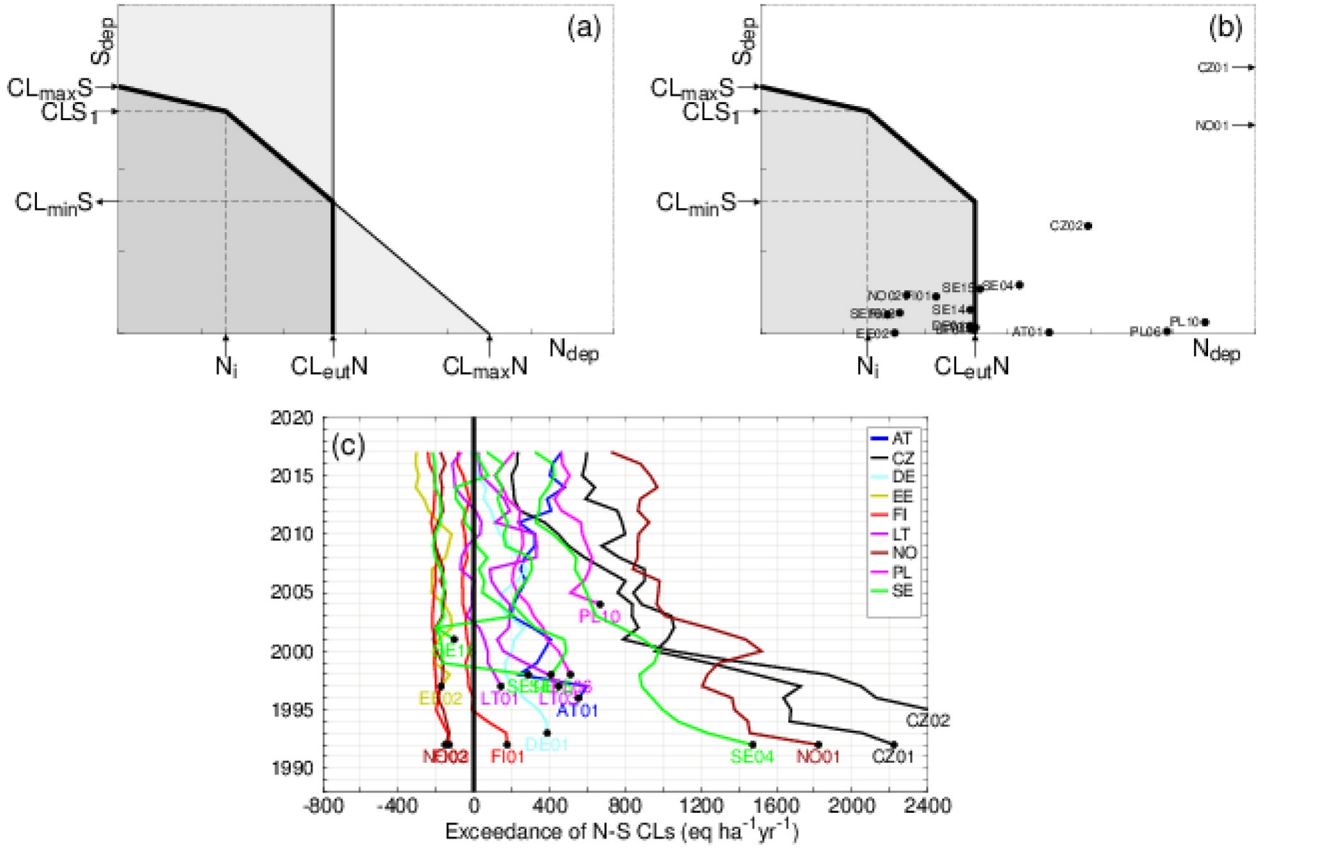

Fig. 4. Exceedance of the single critical load function for N and S: (a) Acidity CL function intersected with the critical load of eutrophication, $CL_{eut}N$, defining the N and S CL function. For N and S depositions in the dark grey area neither acidity nor eutrophication CLs are exceeded, implying that neither the acidity nor the eutrophication criterion is violated; (b) Normalized N-S CLF for 17 ICP-M sites and their depositions in 2017. Note: For two sites the N deposition is too far beyond its respective $CL_{eut}N$; (c) Exceedance of N-S CL function over time at the ICP-IM sites using the total N and S deposition measurements at the sites (3-year moving average). Negative numbers indicate non-exceedance.

critical load function can be found in Posch et al. (2015b). The growing emphasis on biodiversity impacts of air pollutants (especially plant diversity, Dirnböck et al., 2014; Rowe et al., 2017; McDonnell et al., 2020; Wamelink et al., 2020) increases the utility of a combined approach. Dynamic soil models, coupled to statistical plant species niche models and applied with scenarios for climate and deposition, can be used to derive N-S CL functions for plant diversity (e.g. Dirnböck et al., 2018).

3.4. Change in exceedances versus change in water quality

The CL and exceedance calculations are an important source of information for making formal emission reduction agreements under CLRTAP and the EU (De Vries et al., 2015; Grennfelt et al., 2020). Many simplifying assumptions are made in these calculations and it is essential that sites with intensive observations are used to study how the temporal development of the CL exceedance is reflected in the monitored ecosystem effect indicators. A continuous effort to develop the CL concept and reduce uncertainties in the CL modelling approach is also needed. The comprehensive database of the intensively studied ICP IM sites provides important datasets for such efforts.

There is a clear relation between measured runoff water concentrations and fluxes and calculated CL exceedances of eutrophication and acidity at the ICP IM sites (Fig. 5). Generally, the sites with higher exceedance of both Ex_{eut} and Ex_{aci} showed larger decreases in both TIN (Fig. 5a, b) and H^+ (Fig. 5c, d) concentrations and fluxes as an assumed response to decreasing depositions. These results reflect both the European emission/deposition gradient with highest present and

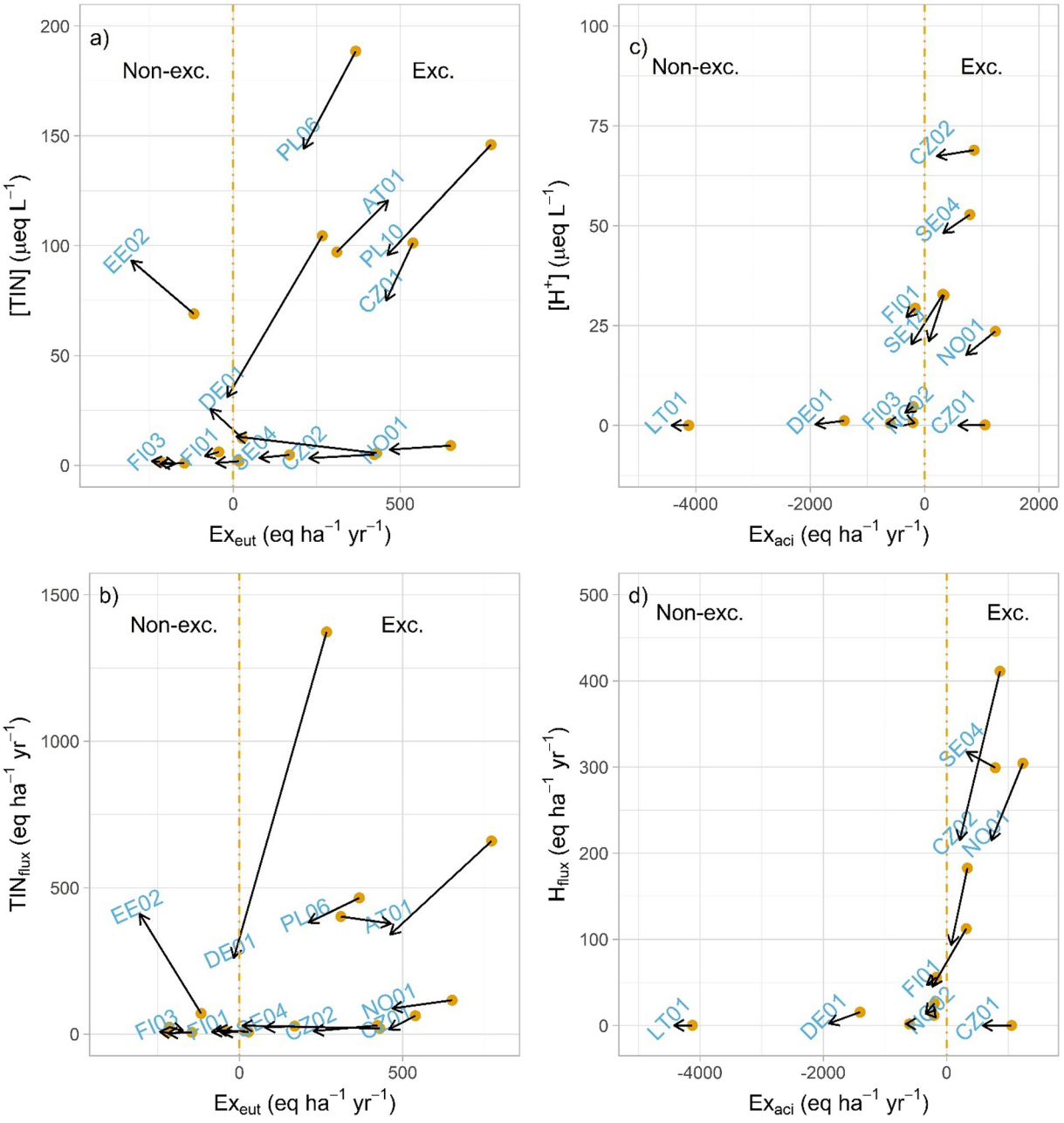

Fig. 5. Relation between runoff water total inorganic nitrogen (TIN) and exceedance of critical loads of eutrophication (a, b) and relation between runoff water hydrogen ions and exceedance of critical loads of acidity (c ,d).TIN concentration (µeq L^{-1}) a) and TIN flux (eq ha^{-1} yr^{-1}) b) versus Ex_{eut} (eq ha^{-1} yr^{-1}) at 16 sites (AT01, CZ01, CZ02, DE01, EE02, FI01, FI03, LT01, NO01, NO02, PL06, PL10, SE04, SE14, SE15, and SE16. Concentration [H^+] (µeq L^{-1}) c) and H^+ flux (eq ha^{-1} yr^{-1}) d) versus exceedance of critical loads of acidity (Ex_{aci}) at 12 relatively less well buffered sites (CZ01, CZ02, DE01, FI01, FI03, LT01, NO01, NO02, SE04, SE15, SE14 and SE16). The arrows represent the change from the period 2000–2002 (yellow circle) to the period 2015–2017 (black arrow head).

cumulative depositions in the central and eastern regions (Fig. 1; Vuorenmaa et al., 2018; Fagerli et al., 2019), as well as the sensitivity of the sites based on the CL calculations. For example, sites DE01 and LT01 have received rather high deposition loads but show non-exceedance of Ex_{aci}, and consequently also small changes in H^+ concentrations and fluxes (Fig. 5c,d). Some of the sites, particularly AT01, EE02 and the two Polish sites (PL06, PL10) have very high acidity CLs (Table 2), so acidification (and exceedance of acidity CLs) has never been an issue of concern.

It should be recognized that catchment processes regulating responses to eutrophying and acidifying deposition are inherently complex, particularly regarding N. The statistically significant increase in TIN concentrations and/or fluxes in runoff observed at sites SE04 and SE14 (Table 2) have at least partly been caused by storm-fellings followed by bark beetle infestations (Löfgren et al., 2011, 2014). According to Vuorenmaa et al. (2018) also increased runoff volume may be a partial cause for the increased NO_3 flux at SE04, but this site is also affected by annually occurring wind throws and bark beetle attacks as well as of a thinning operation in 2012 of the upper part of the catchment (Löfgren, 2019). The site AT01 is a karst catchment with complex hydrological patterns affecting the N leaching processes (Hartmann et al., 2012). Also, site DE01 was affected by a bark beetle infestation in years 1997–2007 (Beudert et al., 2014), but N concentrations and fluxes have decreased again after a period of substantial increase.

The risk of N leaching (mainly concerning NO_3) has also been related to N deposition thresholds and C/N ratios in the topsoil. Several studies have indicated an elevated risk for NO_3 leaching at N deposition levels exceeding ca. 600–700 eq ha^{-1} yr^{-1} (8–10 kg ha^{-1} yr^{-1}) (e.g. Dise and Wright, 1995; Forsius et al., 2001; Wright et al., 2001; Dise et al., 2009). That level of N deposition is most clearly exceeded at ICP IM sites in central Europe and southern Norway, and in these regions the sites also show higher fluxes and concentrations of TIN and NO_3 (Table 3, Fig. 5a, b; see Vuorenmaa et al., 2018 for long-term averages). N processes and leaching are also affected by short- and long-term climatic variations (e.g. Wright et al., 2001, 2006; Vuorenmaa et al., 2018).

As explained above, CL and exceedance calculations are based on steady-state assumptions, easily leading to a conclusion that reducing deposition to (or below) the CL directly removes the risk of "significant harmful effects", and also causing biological recovery. However, several dynamic processes, e.g. soil S adsorption or N immobilisation, can delay reaching these steady-state conditions for very long time periods (decades to centuries) (Wright et al., 2005; Johnson et al., 2018; Posch et al., 2019). These buffering processes cannot be considered in the CL formulation, since they do not influence the steady-state but only the time to reach it. In this context, two generalized past and future development stages of the system have been introduced: 'Damage Delay Time (DDT)' and 'Recovery Delay Time (RDT)'. DDT is the time (in the past) between the first exceedance of a CL and the first violation of the chemical criterion. RDT is the first non-exceedance (after deposition reduction) of that CL and the time when the chemical criterion is no longer violated (see Posch et al., 2019 for details).

While a DDT can hardly be observed for the ICP IM sites (measurements started only when depositions were already high), we demonstrate the concept of RDT using the acidity CLs calculations and empirical observations for two sites (CZ02 and DE01), showing a large reduction in Ex_{aci} but of different sensitivity to acidic deposition (Fig. 6). Site CZ02 (Lysina) barely moves across borders of non-exceedance of the CL and the subsequent non-violation of the chemical criterion (ANC_{limit} = 20 μeq L^{-1}). The less sensitive site DE01 (Forellenbach) has never had any exceedance of acidity CLs or violation of the chemical criterion.

The target load concept is an extension of the CL approach, allowing the determination of both the deposition *and* the point in time (target year) for non-violation of the critical limit (Jenkins et al., 2003; Sullivan et al., 2012; Posch et al., 2019). Despite this advantage, target loads have not yet been directly used in the emission abatement policy processes. The reason is likely the large needs of input data and expertise required to determine target loads compared to CLs, that are based on simpler assumptions. However, a wider use of the target load concept would provide information also on the time needed to reach the desired policy goal for the ecosystem status. Presently available modelling platforms at the ICP IM sites (Dirnböck et al., 2018; Holmberg et al., 2018) would provide a good basis also for detailed target load evaluations, and this is anticipated to be an area of extended work in the future.

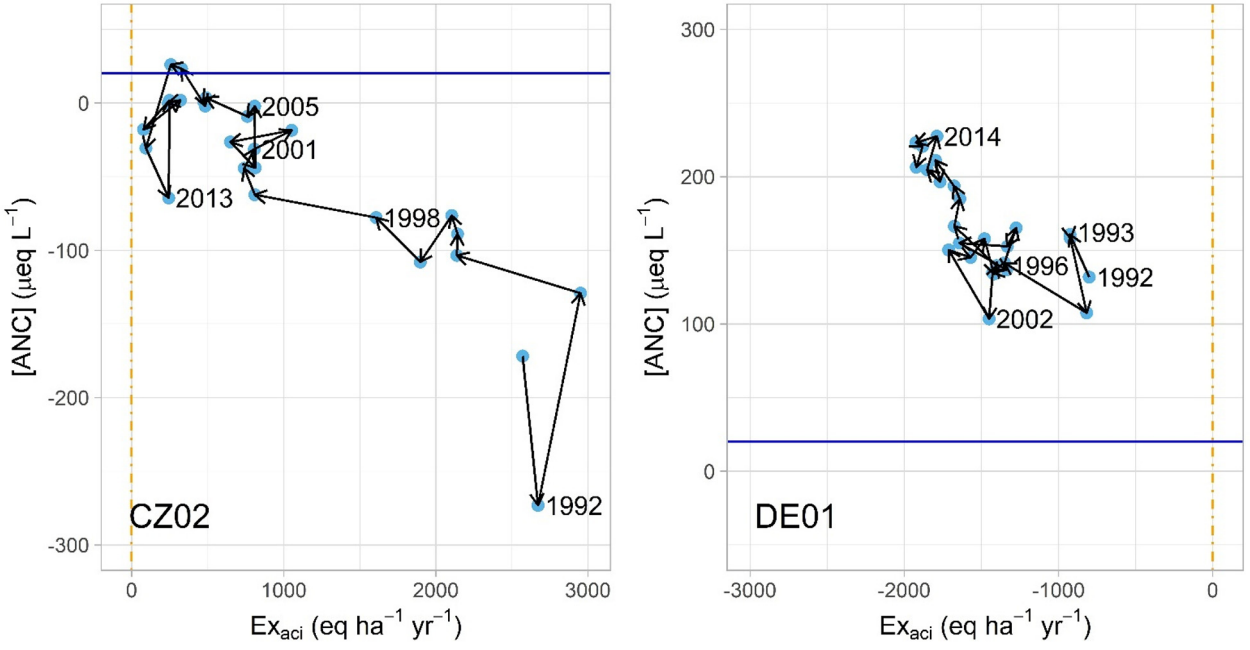

Fig. 6. Response trajectories for sites CZ02 (Lysina) from 1991 to 2017; and DE01 (Forellenbach) from 1992 to 2017. CZ02 barely rises above the chemical criterion ANC_{limit} = 20 μeq L^{-1} in 2010 and 2011. Site DE01 never showed exceedance the acidity CLs or violation of the ANC_{limit}.

3.5. Cumulative exceedance of the critical load of eutrophication versus TIN in runoff water

Both empirical N addition experiments (Moldan and Wright, 2011) and modelling studies (Dirnböck et al., 2017, 2018; Holmberg et al., 2018) have shown that N impacts depend on both the deposition history and current loads. It has therefore been argued that cumulative N deposition would be a better indicator for ecosystem impacts than current deposition. However, this approach also has many uncertainties, such as immobilisation of deposited N into organic matter and fast vs. slow response of sensitive species to N impacts (Rowe et al., 2017).

A compromise between using cumulative total deposition and current deposition, which may either overestimate or underestimate the effects of persistent N, is to calculate deposition above a threshold and for a defined time period. Thus, following Rowe et al. (2017), we compare the recent measured concentration of TIN (averaged over 2015–17 to reduce inter-annual fluctuations) with average positive exceedances of $CL_{eut}N$ over the last 3 years (2015–17, Fig. 7 left) and the last 30 years (1988–2017, Fig. 7 right). The 30-year cumulative exceedance has also been investigated by Rowe et al. (2017) to find a link between observed impacts and a potential cause. Note that average exceedances are shown in Fig. 7, i.e. cumulative exceedances divided by the resp. number of years. As can be seen (Fig. 7 left), the recent 3-year averages are in general lower, indicating that N deposition has gone down over the last years (as $CL_{eut}N$ is independent of time). Sites with higher average/cumulative exceedance of $CL_{eut}N$ generally show higher TIN concentrations, but there is no big difference in the explanatory power between these two quantities (Fig. 7; $r^2 = 0.366$ vs. $r^2 = 0.342$).

We recognise that our study has many sources of uncertainty, including errors in field sampling, analytical methods and data aggregation, as well as assumptions in the actual CL calculations. Many studies have previously evaluated the uncertainty in the CL approach (see Skeffington, 2006) and the potential influence of climate change (e.g. Posch, 2002). Identified sources of uncertainty include soil physical properties, nutrient cycling, deposition estimates and critical limit values (Posch, 2002; Skeffington, 2006; Holmberg et al., 2013; De Vries et al., 2015). For the development of abatement strategies, large-scale applications of CLs and estimates of cost-efficiency are needed (Maas and Grennfelt, 2016; Grennfelt et al., 2020). However, site-based approaches like the present study can improve the scientific basis of the CL concepts, test their performance and quantify uncertainties. The significant reduction in CL exceedances and associated risks of damage to the ICP IM sites is strongly supported by empirical data.

4. Conclusions

The CL methodology has been a key science-based tool for assessing the environmental consequences of air pollution at different spatial scales, ranging from site-specific to continental. Large-scale modelling and mapping of CLs and their exceedance has consequently been used for evaluating the benefits of emission reduction policies, leading to recovery of key ecosystems in Europe. The present study strongly emphasises the value of detailed catchment data for analysing changes in ecosystem processes, and for providing data for developing modelling and assessment concepts. Our updated empirical trend results show that ecosystem (chemical) recovery generally is continuing with an increasing number of statistically significant decreasing trends in S and N compounds and acidity in both deposition and runoff water. The temporal developments of the exceedance of acidity and eutrophication CLs indicated the more effective reductions of S deposition compared to N at the ICP IM sites. We also show that there generally is a consistent relation between our effect indicator (measured runoff water concentrations and fluxes) and calculated CLs exceedances of eutrophication and acidity at the sites. This increases confidence in the widely applied CL methodology. We have also developed and documented novel techniques for displaying CLs and their exceedances using observed site data, and these methodologies can be used for developing and illustrating future science-based emission reduction protocols. The collected data and available modelling tools also provide a good basis for detailed dynamic approaches, such as target load calculations.

Simplifications and uncertainties associated with CL modelling are well acknowledged. Remaining uncertainties include determination of soil properties used for estimating model parameters, processes of nutrient cycling, deposition estimates and critical limit values. Continued work is therefore needed to improve these modelling concepts and to secure the collection of the required long-term detailed ecosystem and experimental data. Dynamic approaches and climate change and air pollution interactions are assumed to receive increasing attention in future work.

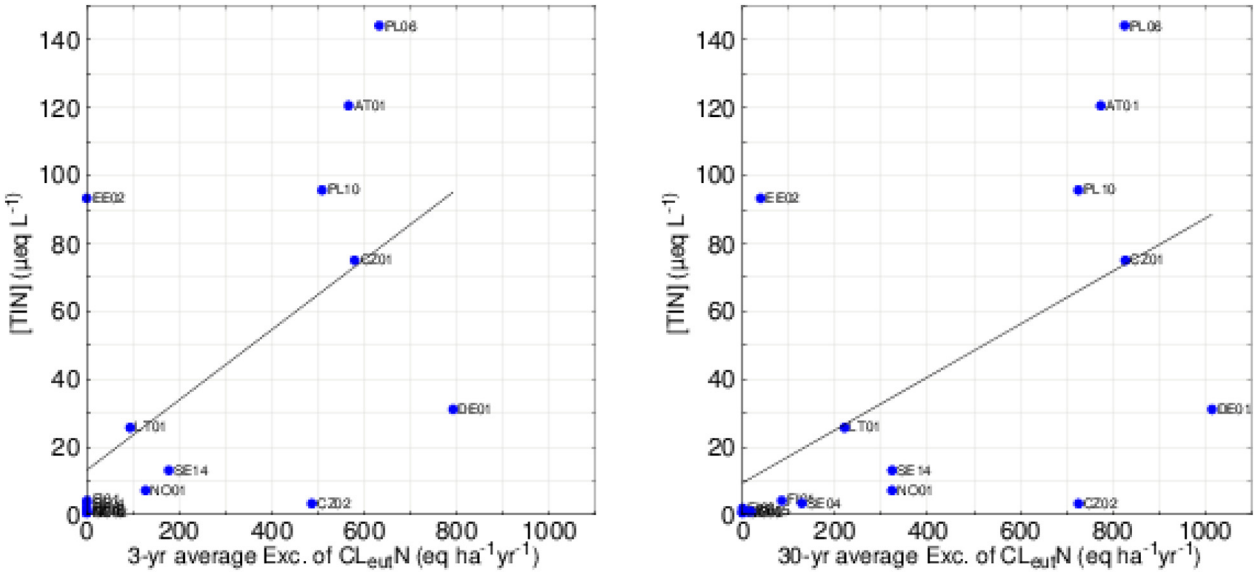

Fig. 7. Average exceedance of $CL_{eut}N$ (in eq ha^{-1} yr^{-1}) vs. observed 2015–17 average observed [TIN] (µeq L^{-1}). Positive exceedances are averaged over 3 years (2015–17; left) and 30 years (1988–2017; right). Also shown are the regression lines (left: $r^2 = 0.366$; right $r^2 = 0.342$).

CRediT authorship contribution statement

Martin Forsius planned the manuscript and had the main responsibility for writing the text. Maximilian Posch and Maria Holmberg performed the critical loads calculations, participated in methods development and provided input to the text. Jussi Vuorenmaa carried out the statistical calculations of the collected data and provided input to the text. Sirpa Kleemola was responsible for the database. Other authors provided data and comments to the manuscript.

Declaration of competing interest

The authors declare that they have no known competing financial interests or personal relationships that could have appeared to influence the work reported in this paper.

Acknowledgements

We would like to thank the LRTAP Convention Trust Fund (grant agreement no. LUA-E910), the European Commission via H2020-project eLTER PLUS (grant agreement no. 871128), the Academy of Finland/Strategic Research Council (grant agreements no. 304467 and 312559), and the Swedish Environmental Protection Agency for financial support of the study. We would also like to thank the national focal points and many national institutions supporting the ICP IM and eLTER work for continued intensive catchment monitoring and data aggregation efforts.

Appendix A. Supplementary data

Supplementary data to this article can be found online at https://doi.org/10.1016/j.scitotenv.2020.141791.

References

Amann, M., Bertok, I., Borken-Kleefeld, J., Cofala, J., Heyes, C., Höglund-Isaksson, L., Klimont, Z., Nguyen, B., Posch, M., Rafaj, P., Sandler, R., Schöpp, W., Wagner, F., Winiwarter, W., 2011. Cost-effective control of air quality and greenhouse gases in Europe: modeling and policy applications. Environ. Model Softw. 26 (12), 1489–1501.

Baker, L.A., Brezonik, P.L., 1988. Dynamic model of in-lake alkalinity generation. Water Resour. Res. 24 (1), 65–74.

Bergström, A.-K., Blomqvist, P., Jansson, M., 2005. Effects of nitrogen deposition on nutrient limitation and phytoplankton biomass in unproductive Swedish lakes. Limnol. Oceanogr. 50, 987–994.

Beudert, B., Bässler, C., Thorn, S., Noss, R., Schröder, B., Dieffenbach-Fries, H., Foullois, N., Müller, Jörg, 2014. Bark beetles increase biodiversity while maintaining drinking water quality. Conserv. Lett. 8, 272–281.

Bobbink, R., Hettelingh, J.-P., 2011. Review and Revision of Empirical Critical Loads and Dose-Response Relationships. Proceedings of an Expert Workshop, Noordwijkerhout 23–24 June 2010. Report 680359002, RIVM, Bilthoven, the Netherlands.

Bobbink, R., Hicks, K., Galloway, J., Spranger, T., Alkemade, R., Ashmore, M., Bustamante, M., Cinderby, S., Davidson, E., Dentener, F., Emmett, B., Erisman, J.W., Fenn, M., Gilliam, F., Nordin, A., Pardo, L., de Vries, W., 2010. Global assessment of nitrogen deposition effects on terrestrial plant diversity: a synthesis. Ecol. Appl. 20, 30–59.

Brakke, D.F., Henriksen, A., Norton, S.A., 1990. A variable F-factor to explain changes in base cation concentrations as a function of strong acid deposition. Verh. Internat. Verein Limnol. 24, 146–149.

De Vries, W., Hettelingh, J.-P., Posch, M. (Eds.), 2015. Critical Loads and Dynamic Risk Assessments: Nitrogen, Acidity and Metals in Terrestrial and Aquatic Ecosystems. Environmental Pollution Series. vol. 25. Springer, Dordrecht. https://doi.org/10.1007/978-94-017-9508-1 ISBN 978-94-017-9507-4.

Dirnböck, T., Grandin, U., Bernhardt-Römermann, M., Beudert, B., Canullo, R., Forsius, M., Grabner, M.T., Holmberg, M., Kleemola, S., Lundin, L., Mirtl, M., Neumann, M., Pompei, E., Salemaa, M., Starlinger, F., Staszewski, T., Uziębło, A.K., 2014. Forest floor vegetation response to nitrogen deposition in Europe. Glob. Chang. Biol. 20, 429–440. https://doi.org/10.1111/gcb.12440.

Dirnböck, T., Foldal, C., Djukic, I., Kobler, J., Haas, E., Kiese, R., Kitzler, B., 2017. Historic nitrogen deposition determines future climate change effects on nitrogen retention in temperate forests. Clim. Chang. 144 (2), 221–235. https://doi.org/10.1007/s10584-017-2024-y.

Dirnböck, T., Pröll, G., Austnes, K., Beloica, J., Beudert, B., Canullo, R., De Marco, A., Fornasier, M.A., Futter, M., Goergen, K., Grandin, U., Holmberg, M., Lindroos, A.J., Mirtl, M., Neirynck, J., Pecka, T., Nieminen, T.M., Nordbakken, J.F., Posch, M., Reinds, G.J., Rowe, E., Salemaa, M., Scheuschner, T., Starlinger, F., Uziębło, A.K., Valinia, S., Weldon, J., Wamelink, W., Forsius, M., 2018. Currently legislated decreases in nitrogen deposition will yield only limited plant species recovery in European forests. Environ. Res. Lett. 13 (2018), 125010. https://doi.org/10.1088/1748-9326/aaf26b.

Dise, N.B., Wright, R.F., 1995. Nitrogen leaching from European forests in relation to nitrogen deposition. For. Ecol. Manag. 71, 153–162.

Dise, N.B., Rothwell, J.J., Gauci, V., van der Salm, C., de Vries, W., 2009. Predicting dissolved inorganic nitrogen leaching in European forests using two independent databases. Sci. Total Environ. 407, 1798–1808.

Duan, L., Xie, S.D., Zhou, Z.P., Hao, J.M., 2000a. Critical loads of acid deposition on soil in China. Water Air Soil Pollut. 118, 35–51.

Duan, L., Hao, J., Xie, S., Du, K., 2000b. Critical loads of acidity for surface waters in China. Sci. Total Environ. 246, 1–10.

Dupre, C., Stevens, C.J., Ranke, T., et al., 2010. Changes in species richness and composition in European acidic grasslands over the past 70 years: the contribution of cumulative atmospheric nitrogen deposition. Glob. Chang. Biol. 16, 344–357.

Fagerli, H., Tsyro, S., Denby, B.R., et al., 2016. Transboundary particulate matter, photo-oxidants, acidifying and eutrophying components. EMEP Report 1/2016. Norwegian Meteorological Institute, Oslo.

Fagerli, H., Tsyro, S., Jonson, J.E., et al., 2019. Transboundary particulate matter, photo-oxidants, acidifying and eutrophying components. EMEP Report 1/2019. Norwegian Meteorological Institute, Oslo.

Forsius, M., Kleemola, S., Vuorenmaa, J., Syri, S., 2001. Fluxes and trends of nitrogen and sulphur compounds at integrated monitoring sites in Europe. Water Air Soil Poll 130, 1641–1648.

Forsius, M., Kleemola, S., Starr, M., 2005. Proton budgets for a network of European forested catchments: impacts of nitrogen and sulphur deposition. Ecol. Indic. 5, 73–83.

Forsius, M., Posch, M., Aherne, J., Reinds, G.J., Christensen, J., Hole, L., 2010. Assessing the impacts of long-range sulfur and nitrogen deposition on arctic and sub-arctic ecosystems. Ambio 39, 136–147. https://doi.org/10.1007/s13280-010-0022-7.

Garmo, Ø.A., Skjelkvåle, B.L., de Wit, H.A., Colombo, L., Curtis, C., Fölster, J., Hoffmann, A., Hruška, J., Høgåsen, T., Jeffries, D.S., Keller, W.B., Krám, P., Majer, V., Monteith, D.T., Paterson, A.M., Rogora, M., Rzychon, D., Steingruber, S., Stoddard, J.L., Vuorenmaa, J., Worsztynowicz, A., 2014. Trends in surface water chemistry in acidified areas in Europe and North America from 1990 to 2008. Water Air Soil Pollut. 225, 1880. https://doi.org/10.1007/s11270-014-1880-6.

Gilbert, R.O., 1987. Statistical Methods for Environmental Pollution Monitoring. John Wiley and sons, New York.

Grennfelt, P., Engleryd, A., Forsius, M., Hov, Ø., Rodhe, H., Cowling, E., 2020. Acid rain and air pollution– 50 years of progress in environmental science and policy. Ambio 49, 849–864. https://doi.org/10.1007/s13280-019-01244-4.

Hartmann, A., Kralik, M., Humer, F., et al., 2012. Identification of a karst system's intrinsic hydrodynamic parameters: upscaling from single springs to the whole aquifer. Environ. Earth Sci. 65, 2377–2389. https://doi.org/10.1007/s12665-011-1033-9.

Henriksen, A., Posch, M., 2001. Steady-state models for calculating critical loads of acidity for surface waters. Water Air Soil Pollut. Focus 1, 375–398.

Hesthagen, T., Fjellheim, A., Schartau, A.K., Wright, R.F., Saksgard, R., Rosseland, B.O., 2011. Chemical and biological recovery of Lake Saudlandsvatn, a formerly highly acidified lake in southernmost Norway, in response to decreased acid deposition. Sci. Total Environ. 409, 2908–2916.

Hettelingh, J.-P., Posch, M., Slootweg, J., 2017. European Critical Loads: Database, Biodiversity and Ecosystems at Risk: CCE Final Report 2017. RIVM Report 2017–0155, Coordination Centre for Effects, Bilthoven, Netherlands. , p. 204 ISBN 978-90-6960-288-2. 10.21945/rivm-2017-0155.

Holmberg, M., Vuorenmaa, J., Posch, M., Forsius, M., Lundin, L., Kleemola, S., Augustaitis, A., Beudert, B., de Wit, H.A., Dirnböck, T., Evans, C.D., Frey, J., Grandin, U., Indriksone, I., Krám, P., Pompei, E., Schulte-Bisping, H., Srybnyn, A., Vána, M., 2013. Relationship between critical load exceedances and empirical impact indicators at integrated monitoring sites across Europe. Ecol. Indic. 24, 256–265. https://doi.org/10.1016/j.ecolind.2012.06.013.

Holmberg, M., Aherne, J., Austnes, K., Beloica, J., DeMarco, A., Dirnböck, T., Fornasier, M.F., Goergen, K., Futter, M.J., Lindroos, A.-J., Krám, P., Neirynck, J., Nieminen, T.M., Pecka, T., Posch, M., Pröll, G., Rowe, E.C., Scheuschner, T., Schlutow, A., Valinia, S., Forsius, M., 2018. Modelling study of soil C, N and pH response to air pollution and climate change using European LTER site observations. Sci. Tot. Env. 640–641, 387–399. https://doi.org/10.1007/s11270-014-1880-6.

Jenkins, A., Camarero, L., Cosby, B.J., Ferrier, R.C., Forsius, M., Helliwell, R.C., Kopáček, J., Majer, V., Moldan, F., Posch, M., Rogora, M., Schöpp, W., Wright, R.F., 2003. A modelling assessment of acidification and recovery of European surface waters. Hydrol. Earth Syst. Sci. 7 (4), 447–455. https://doi.org/10.5194/hess-7-447-2003.

Johnson, J., Graf Pannatier, E., Carnicelli, S., et al., 2018. The response of soil solution chemistry in European forests to decreasing acid deposition. Glob. Chang. Biol. 24, 3603–3619. https://doi.org/10.1111/gcb.14156.

Jonard, M., Fürst, A., Verstraeten, A., Thimonier, A., Timmermann, V., Potočić, N., Waldner, P., Benham, S., Hansen, K., Merilä, P., Ponette, Q., De La Cruz, A.C., Roskams, P., Nicolas, M., Croisé, L., Ingerslev, M., Matteucci, G., Decinti, B., Bascietto, M., Rautio, P., 2015. Tree mineral nutrition is deteriorating in Europe. Glob. Chang. Biol. 21, 418–430. https://doi.org/10.1111/gcb.12657.

Josipovic, M., Annegarn, H.J., Kneen, M.A., Pienaar, J.J., Piketh, S.J., 2011. Atmospheric dry and wet deposition of sulphur and nitrogen species and assessment of critical loads of acidic deposition exceedance in South Africa. S. Afr. J. Sci. 107 (3/4), 478. https://doi.org/10.4102/sajs.v107i3/4.478.

Karltun, E., Stendahl, J., Lundin, L., 2003. Acid-base Status and Changes in Swedish Forest Soils. 142(18). Agerlid, G, Soil and surface water acidification in theory and practice. The Royal Swedish Academy of Agriculture and Forestry Stockholm, KSLAT, pp. 31–36 ISBN 91–89379-61-6. https://www.ksla.se/publikationer/kslat/kslat-18-2003/.

Kaste, Ø., Dillon, P.J., 2003. Inorganic nitrogen retention in acid-sensitive lakes in southern Norway and southern Ontario, Canada - a comparison of mass balance data with an empirical N retention model. Hydrol. Proc. 17, 2393–2407.
Lawrence, G.B., Hazlett, P.W., Fernandez, I.J., Ouimet, R., Bailey, S.W., Shortle, W.C., Smith, K.T., Antidormi, M.R., 2015. Declining acidic deposition begins reversal of forest-soil acidification in the Northeastern U.S. and Eastern Canada. Environmental Science & Technology 49, 13103–13111. https://doi.org/10.1021/acs.est.5b02904.
Liang, T., Aherne, J., 2019. Critical loads of acidity and exceedances for 1138 lakes and ponds in the Canadian Arctic. Sci. Total Environ. 652, 1424–1434. https://doi.org/10.1016/j.scitotenv.2018.10.330.
Libiseller, C., Grimvall, A., 2002. Performance of partial Mann-Kendall tests for trend detection in the presence of covariates. Environmetrics 13, 71–84.
Lien, L., Raddum, G.G., Fjellheim, A., Henriksen, A., 1996. A critical limit for acid neutralizing capacity in Norwegian surface waters, based on new analyses of fish and invertebrate responses. Sci. Total Environ. 177, 173–193.
Löfgren, S., 2019. Integrated Monitoring of the Environmental Status in Swedish Forest Ecosystems – IM. Annual Report for 2018. Dept. Aquatic Sciences and Assessment, SLU Report 2019:7, 34 pp + Appendix. In Swedish. English Summary https://pub.epsilon.slu.se/16519/1/lofgren_s_191217.pdf.
Löfgren, S., Aastrup, M., Bringmark, L., Hultberg, H., Lewin-Pihlblad, L., Lundin, L., Karlsson, G.P., Thunholm, B., 2011. Recovery of soil water, groundwater, and streamwater from acidification at the Swedish integrated monitoring catchments. Ambio 40, 836–856. https://doi.org/10.1007/s13280-011-0207-8.
Löfgren, S., Stendera, S., Grandin, U., 2014. Long-term effects on nitrogen and benthic fauna of extreme climatic events – examples from two headwater streams. Ambio 43, 58–76. https://doi.org/10.1007/s13280-014-0562-3.
Lund, E., Garmo, O.A., de Wit, H.A., Kristensen, T., Hawley, K.L., Wright, R.F., 2018. Reduced acid deposition leads to a new start for Brown Trout (*Salmo trutta*) in an acidified lake in southern Norway. Water Air and Soil Pollution 229, 368. https://doi.org/10.1007/s11270-018-4013-9.
Maas, R., Grennfelt, P. (Eds.), 2016. Towards Cleaner Air. 2016. EMEP Steering Body and Working Group on Effects of the Convention on Long-Range Transboundary Air Pollution, Oslo Scientific Assessment Report. (50 pp).
Manual for Integrated Monitoring, 2013. Finnish Environment Institute, ICP IM Programme Centre, Helsinki, Finland. www.syke.fi/nature/icpim, Accessed: 3 April 2020.
Mapping Manual, d. German Environment Agency, Coordination Centre for Effects. www.icpmapping.org. (Accessed 3 April 2020). .
McDonnell, T.C., Reinds, G.J., Wamelink, G.W.W., Goedhart, P.W., Posch, M., Sullivan, T.J., Clark, C.M., 2020. Threshold effects of air pollution and climate change on understory plant communities at forested sites in the eastern United States. Environ. Pollut. 262, 114351. https://doi.org/10.1016/j.envpol.2020.114351.
Mirtl, M., Borer, E.T., Djukic, I., Forsius, M., Haubold, H., Hugo, W., Jourdan, J., Lindenmayer, D., McDowell, W.H., Muraoka, H., Orenstein, D.E., Pauw, J.C., Peterseil, J., Shibata, H., Wohner, C., Yu, X., Haase, P., 2018. Genesis, goals and achievements of long-term ecological research at the global scale: a critical review of ILTER and future directions. Sci. Total Environ. 626, 1439–1462. https://doi.org/10.1016/j.scitotenv.2017.12.001.
Mitchell, M.J., Driscoll, C.T., McHale, P.J., Roy, K.M., Dong, Z., 2013. Lake/watershed sulfur budgets and their response to decreases in atmospheric sulfur deposition: watershed and climate controls. Hydrol. Process. 27, 710–720.
Moldan, F., Wright, R.F., 2011. Nitrogen leaching and acidification during 19 years of NH_4NO_3 additions to a coniferous-forested catchment at Gardsjon, Sweden (NITREX). Environ. Pollut. 159, 431–440.
Monteith, D.T., Hildrew, A.G., Flower, R.J., Raven, P.J., Beaumont, W.R.B., Collen, P., et al., 2005. Biological responses to the chemical recovery of acidified fresh waters in the UK. Environ. Pollut. 137, 83–101.
Critical loads for sulphur and nitrogen. In: Nilsson, J., Grennfelt, P. (Eds.), Environmental Report 1988:15. Copenhagen, Nordic Council of Ministers.
Ouimet, R., Arp, P.A., Watmough, S.A., Aherne, J., Demerchant, I., 2006. Determination and mapping critical loads of acidity and exceedances for upland forest soils in Eastern Canada. Water Air Soil Pollut. 172, 57–66.
Oulehle, F., Chuman, T., Hruška, J., Krám, P., McDowell, W.H., Myška, O., Navrátil, T., Tesar, M., 2017. Recovery from acidification alters concentrations and fluxes of solutes from Czech catchments. Biogeochemistry 132, 251–272. https://doi.org/10.1007/s10533-017-0298-9.
Pardo, L.H., Fenn, M.E., Goodale, C.L., Geiser, L.H., Driscoll, C.T., Allen, E.B., Baron, J.S., Bobbink, R., Bowman, W.D., Clark, C.M., Emmett, B., Gilliam, F.S., Greaver, T.L., Hall, S.J., Lilleskov, E.A., Liu, L., Lynch, J.A., Nadelhoffer, K.J., Perakis, S.S., Robin- Abbott, M.J., Stoddard, J.L., Weathers, K.C., Dennis, R.L., 2011. Effects of nitrogen deposition and empirical nitrogen critical loads for ecoregions of the United States. Ecol. Appl. 21 (8), 3049–3082.
Posch, M., 2002. Impacts of climate change on critical loads and their exceedances in Europe. Environ. Sci. Pol. 5 (4), 307–317.
Posch, M., Kämäri, J., Forsius, M., Henriksen, A., Wilander, A., 1997. Exceedance of critical loads for lakes in Finland, Norway and Sweden: reduction requirements for acidifying nitrogen and sulfur deposition. Environ. Management 21 (2), 291–304.
Posch, M., Aherne, J., Forsius, M., Rask, M., 2012. Past, present and future exceedance of critical loads of acidity for surface waters in Finland. Environ. Sci. Technol. 46, 4507–4514. https://pubs.acs.org/doi/10.1021/es300332r.
Posch, M., De Vries, W., Sverdrup, H.U., 2015a. Mass balance models to derive critical loads of nitrogen and acidity for terrestrial and aquatic ecosystems. In: Critical Loads and Dynamic Risk Assessments: Nitrogen, Acidity and Metals in Terrestrial and Aquatic Ecosystems; De Vries, W., Hettelingh, J.-P., Posch, M. (Eds.). Springer: Dordrecht 2015, 171–205.
Posch, M., Duan, L., Reinds, G.J., Zhao, Y., 2015b. Critical loads of nitrogen and sulphur to avert acidification and eutrophication in Europe and China. Landsc. Ecol. 30 (3), 487–499. https://doi.org/10.1007/s10980-014-0123-y.
Posch, M., Aherne, J., Moldan, F., Evans, C.D., Forsius, M., Larssen, T., Helliwell, R.C., Cosby, B.J., 2019. Dynamic modeling and target loads of sulfur and nitrogen for surface waters in Finland, Norway, Sweden, and the United Kingdom. Environ. Sci. Technol. 53 (9), 5062–5070. https://doi.org/10.1021/acs.est.8b06356.
Rowe, E.C., Jones, L., Dise, N.B., et al., 2017. Metrics for evaluating the ecological benefits of decreased nitrogen deposition. Biol. Conserv. 212 (2017), 454–463. https://doi.org/10.1016/j.biocon.2016.11.022.
Schmitz, A., Sanders, T., Bolte, A., Bussotti, F., Dirnböck, T., Johnson, J., Penuelas, J., Pollastrini, M., Prescher, A.-K., Sardans, J., Verstraeten, A., de Vries, W., 2019. Responses of forest ecosystems in Europe to decreasing nitrogen deposition. Environ. Pollut. 244, 980–994. https://doi.org/10.1016/j.envpol.2018.09.101.
Schöpp, W., Posch, M., Mylona, S., Johansson, M., 2003. Long-term development of acid deposition (1880-2030) in sensitive freshwater regions in Europe. Hydrol. Earth Syst. Sci. 7 (4), 436–446. https://doi.org/10.5194/hess-7-436-2003.
Sen, P.K., 1968. Estimates of the regression coefficient based on Kendall's tau. J. Am. Stat. Assoc. 63, 1379–1389.
Skeffington, R.A., 2006. Quantifying uncertainty in critical loads: (A) literature review. Water Air Soil Pollut. 169, 3–24.
Staude, I.R., Waller, D.M., Bernhardt-Römermann, M., et al., 2020. Replacements of small- by large-ranged species scale up to diversity loss in Europe's temperate forest biome. Nat. Ecol. Evol. https://doi.org/10.1038/s41559-020-1176-8.
Stevens, C.J., Dupre, C., Dorland, E., et al., 2010. Nitrogen deposition threatens species richness of grasslands across Europe. Env. Poll. 158, 2940–2945.
Sullivan, T.J., Cosby, B.J., Driscoll, C.T., McDonnell, T.C., Herlihy, A.T., Burns, D.A., 2012. Target loads of atmospheric sulfur and nitrogen deposition for protection of acid sensitive aquatic resources in the Adirondack Mountains, New York. Water Resour. Res. 48 (1), W01547.
Sullivan, T.J., Driscoll, C.T., Beier, C.M., Burtraw, D., Fernandez, I.J., Galloway, J.N., Gay, D.A., Goodale, C.A., Likensi, G.E., Lovett, G.M., Watmough, S.A., 2018. Air pollution success stories in the United States: the value of long-term observations. Environ Sci Policy 84, 69–73. https://doi.org/10.1016/j.envsci.2018.02.016.
Sutton, M., Oenema, O., Erisman, J.W., Leip, A., van Grinsven, H., Winiwarter, W., 2011. Too much of a good thing. Nature 472, 159–161. https://doi.org/10.1038/472159a.
Van der Linde, S., Suz, L.M., Orme, C.D.L., et al., 2018. Environment and host as large-scale controls of ectomycorrhizal fungi. Nature 558, 243–248. https://doi.org/10.1038/s41586-018-0189-9.
Vrba, J., Kopáček, J., Fott, J., Kohout, L., Nedbalova, L., Prazakova, M., et al., 2003. Long-term studies (1871-2000) on acidification and recovery of lakes in the Bohemian Forest (central Europe). Sci. Total Environ. 310, 73–85.
Vuorenmaa, J., Augustaitis, A., Beudert, B., Clarke, N., de Wit, H., Dirnböck, T., Frey, J., Forsius, M., Indriksone, I., Kleemola, S., Kobler, J., Krám, P., Lindroos, A.-J., Lundin, L., Ruoho-Airola, T., Ukonmaanaho, L., Váňa, M., 2017. Long-term sulphate and inorganic nitrogen mass balance budgets in European ICP integrated monitoring catchments (1990–2012). Ecol. Indic. 76, 15–29. https://doi.org/10.1016/j.ecolind.2016.12.040.
Vuorenmaa, J., Augustaitis, A., Beudert, B., Bochenek, W., Clarke, N., de Wit, H., Dirnböck, T., Frey, J., Hakola, H.., Indriksone, I., Kleemola, S., Kobler, J., Krám, P., Lindroos, A.-J., Lundin, L., Löfgren, S., Marchetto, A., Pecka, T., Schulte-Bisping, H., Skotak, K., Srybny, A., Szpikowski, J., Ukonmaanaho, L., Váňa, M., Åkerblom, S., Forsius, M., 2018. Long-term changes (1990–2015) in the atmospheric deposition and runoff water chemistry of sulphate, inorganic nitrogen and acidity for forested catchments in Europe in relation to changes in emissions and hydrometeorological conditions. Sci. Total Environ. 625, 1129–1145. https://doi.org/10.1016/j.scitotenv.2017.12.245.
Wamelink, G.W.W., Mol-Dijkstra, J.P., Reinds, G.J., Voogd, J.C., Bonten, L.T.C., Posch, M., Hennekens, S.M., De Vries, W., 2020. Prediction of plant species occurrence as affected by nitrogen deposition and climate change on a European scale. Environ. Pollut. 266 (2), 115257. https://doi.org/10.1016/j.envpol.2020.115257.
Wright, R.F., Alewell, C., Cullen, J.M., Evans, C.D., Marchetto, A., Moldan, F., Prechtel, A., Rogora, M., 2001. Trends in nitrogen deposition and leaching in acid-sensitive streams in Europe. Hydrol. Earth Syst. Sci. 5, 299–310.
Wright, R.F., Larssen, T., Camarero, L., Cosby, B.J., Ferrier, R.C., Helliwell, R., Forsius, M., Jenkins, A., Kopáček, J., Majer, V., Moldan, F., Posch, M., Rogora, M., Schöpp, W., 2005. Recovery of acidified European surface waters. Environ. Sci. Technol. 39, 64A–72A. https://doi.org/10.1021/es0531778.
Wright, R.F., Aherne, J., Bishop, K., Camarero, L., Cosby, B.J., Erlandsson, M., Evans, C.D., Forsius, M., Hardekopf, D., Helliwell, R., Hruska, J., Jenkins, A., Moldan, F., Posch, M., Rogora, M., 2006. Modelling the effect of climate change on recovery of acidified freshwaters: relative sensitivity of individual processes in the MAGIC model. Sci. Total Environ. 365, 154–166. https://doi.org/10.1016/j.scitotenv.2006.02.042.
Zhao, Y., Duan, L., Larssen, T., Hu, L.H., Hao, J.M., 2007. Simultaneous assessment of depositions of base cations, sulfur and nitrogen using an extended critical load function for acidification. Environ. Sci. Technol. 41, 1815–1820. https://doi.org/10.1021/es060380+.